JOURNAL OF AIRCRAFT
Vol. 37, No. 4, July–August 2000

Flow Control for an Airfoil with Leading-Edge Rotation: An Experimental Study

Ahmed Z. Al-Garni,* Abdullah M. Al-Garni,† Saad A. Ahmed,‡ and Ahmet Z. Sahin‡
King Fahd University of Petroleum and Minerals, Dhahran 31261, Saudi Arabia

An experimental investigation has been conducted on a two-dimensional NACA 0024 airfoil equipped with a leading-edge rotating cylinder. The airfoil was tested for different values of leading-edge rotations and flap deflection angles. The effects of the angle of attack α, the cylinder surface velocity ratio U_c/U, and the flap deflection angle δ on lift and drag coefficients, the size of the separated flow region, and the stall angle of attack are included. The effect of U_c/U on the boundary-layer growth and turbulence intensity are also shown. Experimental results, for example, showed that the leading-edge rotating cylinder increases the lift coefficient of a NACA 0024 airfoil from 0.85 at $U_c/U = 0$ to 1.63 at $U_c/U = 4$ and delays the stall angle of attack by about 160%. Smoke-wire flow visualization results were also used to demonstrate the strong effect of the leading-edge rotating cylinder on the size of the recirculation region.

Nomenclature

C_D	= drag coefficient
C_L	= lift coefficient
L/D	= lift-to-drag ratio
U	= freestream mean velocity, m/s
U_c	= cylinder tangential velocity, m/s
U_c/U	= cylinder surface velocity ratio
u	= mean velocity inside the boundary layer at a specific location, m/s
u'	= root mean square values of velocity fluctuations along x, m/s
u'/U	= turbulence intensity
α	= angle of attack, deg
δ	= flap deflection angle, deg

Subscripts

c	= cylinder
max	= maximum
R	= required for flow reattachment

Introduction

THE problem of boundary-layer control is very important in the field of aerodynamics and hydrodynamics. Boundary-layer control is essential for current wing design technology to increase lift, lift-to-drag ratio, and stall angle of attack. Several methods, such as suction and blowing, have been developed and reported for controlling boundary-layer flow. Although interest in boundary-layer control has increased, little is known about the use of a moving surface to control the boundary layer. Several authors, including Schlichting[1] and Chang,[2] have reviewed a vast body of literature pertaining to boundary-layer control. The effects of a rotating cylinder in a water channel at various cylinder peripheral speeds was investigated by Prandtl and Tietjens.[3]

The application of a clockwise rotating cylinder on the upper surface of an airfoil wing was investigated by Alvarez-Calderon and Arnold.[4] Their investigation covers a vertical takeoff and landing configuration and a short takeoff and landing (STOL) configuration. Results showed that the angle-of-attack range, with attached flows, was substantially doubled and that large flap deflections on the order of 90 deg, with attached flows, were possible. Of the same interest is the flight tests of a flap with a rotating leading edge on a North American Rockwell YOV-10A twin-engine aircraft,[5,6] where the rotating cylinder flap was used to control boundary-layer flow and to improve aerodynamic performance for STOL-type aircraft. The flight test was conducted at speeds of 29–31 m/s and angles of attack up to −8-deg landing approaches that corresponded to a lift coefficient of about 4.3.

Tennant[7] applied the moving wall to an airflow through a diffuser with a step change in area. The diffuser incorporated rotating cylinders to form a part of its wall at the station where the area change took place. Experimental results showed no separation for the appropriate ratio of the moving surface to the diffuser inlet velocity, and the moving surface provided a high area ratio diffuser with a short overall length.

Johnson et al.[8] conducted tests on a symmetrical lifting body with a leading-edge rotating cylinder. The angle of attack, in their study, was limited to 15 deg, and the cylinder speed necessary to reattach the flow was determined. Their study included the effect of the gap between the rotating and fixed surfaces on the effectiveness of the boundary-layer control technique. They concluded that the gap should be kept at its minimum value to minimize the cylinder speed required for effective boundary-layer control.

Circulation control for a symmetrical airfoil with a rotating cylinder forming its trailing edge was presented by Tennant et al.[9] The lift coefficient reached 1.2 with $U_c/U = 3$ at $\alpha = 0$ deg. The lift coefficient and the stagnation point location were found to be linear functions of the cylinder surface velocity ratio U_c/U. In Refs. 10 and 11, the region of transition from a fixed wall to a moving wall was analyzed, and the physical gap between surfaces was ignored by assuming all of the acceleration effects of the wall occurred in a fixed streamwise span.

Sayers[12] presented lift coefficients and stall angles of a rudder with a leading-edge rotating cylinder. Results of the study showed that the leading-edge rotating cylinder increases the lift coefficient and stall angle and, thus, increases the maneuverability of a vessel fitted with such a rudder.

Hassan and Sankar[13] conducted a numerical and experimental study to investigate the effects of forebody boundary-induced vorticity on the development of the laminar/turbulent boundary layers over modified NACA 0012 and NACA 63-218 airfoils with leading-edge rotation. They utilized an implicit finite difference procedure to solve the two-dimensional compressible full Reynolds-averaged Navier–Stokes equations on a body-fitted curvilinear coordinate system. The study presented the effects of varying the circumferential

Received 8 October 1999; revision received 8 October 1999; accepted for publication 7 February 2000.

*Associate Professor, Aerospace Laboratory, Aerospace Engineering Program and Director. Senior Member AIAA.
†Graduate Assistant, Department of Mechanical Engineering.
‡Associate Professor, Department of Mechanical Engineering.

speed on the location of point(s) of the laminar and/or turbulent separation, the size of the separated flow region above the airfoil, the strength and location of shock waves, and the computed sectional lift coefficients. Qualitative comparisons with smoke-wire flow visualization results were presented.

Brooks[14] conducted an experimental investigation of a hydrofoil with rotating cylinders at the leading or trailing edge. The gap between the rotating cylinder and the fixed surface was about 1.5 mm, which is quite large. His results showed that the trailing-edge rotating cylinder is more effective than the leading-edge rotating cylinder in attaining high lift values.

Modi et al.[15,16] presented a comprehensive wind-tunnel test program involving a family of airfoils such as NACA 63-218 and Joukowsky with one or more cylinders forming the moving surface(s). Their results suggested that the leading-edge rotating cylinder increases the maximum lift coefficient and delays the stall angle of attack by 2.73 and 48 deg, respectively. The study also showed that an increase in U_c/U to a value greater than 4 does not yield any additional benefit. Also, in a different paper, Modi et al.[17] showed that using rotating cylinders results in increasing the maximum lift coefficient by more than 150% and delays the stall to a value of $\alpha = 44$ deg.

The objective of the current paper is to present results for the NACA 0024 airfoil equipped with a leading-edge rotating cylinder. The investigation addresses the effects of the angle of attack α, the surface velocity ratio for the airfoil U_c/U, and the flap deflection angle δ on the lift and drag coefficients, the size of the separated flow region, and the stall angle of attack. It also shows the effect of the surface velocity U_c/U on the boundary-layer velocity profiles and the turbulence intensity. Smoke-wire flow visualization was used to observe the effects of the rotating leading-edge cylinder on the size of the recirculation region.

Experimental Setup and Measuring Technique

Wind Tunnel and Model

Tests were conducted in a low-speed, low-turbulence, open-return-type wind tunnel where the airspeed can be varied from 1 to 40 m/s with a turbulence intensity of less than 1%. The tunnel is powered by a 5.8-kW motor that drives a centrifugal fan. The test section has a cross section of 0.8×0.6 m and is 2.6 m long. It is designed with large plexiglass windows on the top and sides to provide adequate illumination and viewing for visualization studies. A Betz micromanometer with an accuracy of 0.2 mm of water was used to measure the pressure distribution over the surface of the airfoil. The spatial variation of the velocity in the test section was less than 0.5%.

The wind-tunnel model, NACA 0024 airfoil with a 0.2-m chord and 0.048 m maximum thickness spanned the tunnel test section to emulate two-dimensional flow conditions. A plain flap with a chord of 40 mm was placed at the trailing edge of the airfoil. The aspect ratio of the airfoil is 3. Because a large gap between the rotating cylinder and the remaining stationary part of the wing would decrease the effectiveness of the rotating cylinder,[11] the clearance was kept within 0.5 mm. A total of 24 static pressure taps were distributed chordwise along the suction and pressure sides (at the midspan point of the airfoil except on the moving surface). The model was made from wood and painted black to minimize light reflections. A schematic diagram and photograph of the model are shown in Fig. 1.

A 25-mm-diam solid steel cylinder was mounted between two high-speed ball bearings and driven by a variable speed electric motor (1.0 hp, 15 A) mounted outside the tunnel and attached to the cylinder by a standard coupling. The maximum speed of the motor was 14,400 rpm, which was measured using an optical-digital tachometer.

Measurements were conducted at a freestream velocity of 5 m/s. The angle of attack and flap deflection angles were varied from 0 to 40 deg and from 0 to 30 deg, respectively. Different angular speeds (0–14,400 rpm), corresponding to $U_c/U = 0$–4, were directly imparted to the leading-edge cylinder. The Reynolds number was 6.5×10^4 based on the model chord. The aerodynamic forces were calculated by the integration of measured static pressures over the fixed wall portion of the model assuming the skin-friction drag is small compared to the pressure drag.

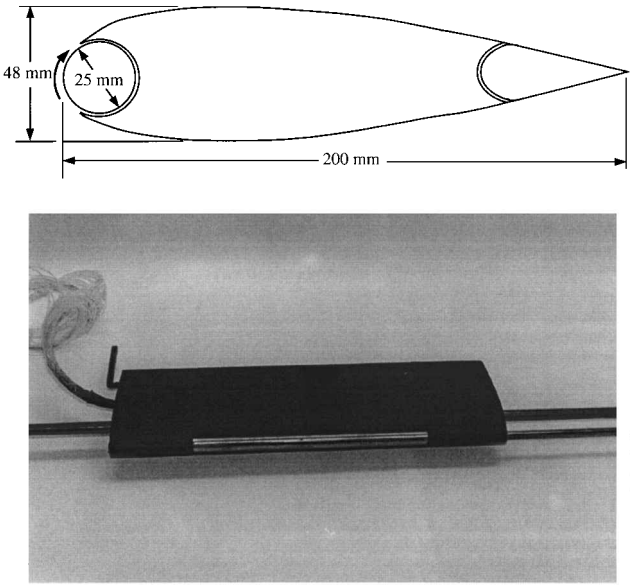

Fig. 1 Schematic of leading-edge rotating cylinder airfoil NACA 0024.

The maximum uncertainty in pressure measurements is about ±4%, whereas the maximum statistical uncertainty for the mean velocity is about ±0.5%. Also, the errors in calculating the lift and drag coefficients are less than ±8 and ±10%, respectively.

Boundary-Layer Measurements

Velocity fluctuations were measured using a miniature single hot-wire probe (DISA 55P15) made of platinum-coated tungsten with a nominal diameter of 0.005 mm and a sensing element length of 1.25 mm. A two-dimensional traverse mechanism with a step of 0.025 mm was used to survey the velocity fluctuations in the vicinity of the airfoil surface. The probe was connected to a constant temperature anemometer (TSI Model IFA 100). The analog outputs from the anemometer were conditioned (offset, gain, and filter), simultaneously digitized, and sent to a computer A/D converter (TSI Model IFA 200 with Model 6260). The digitized data were then deconditioned, corrected for temperature, and converted into velocities using a fourth-order polynomial. The data were stored on the computer, and turbulence quantities such as the mean and turbulence intensities were computed.

Flow Visualization Method

A smoke wire was used to visualize the flow around the model. A 0.1 mm-diam Nichrome smoke wire was placed vertically at 40 cm ahead of the model's leading edge at the midspan point.[18] The wire was coated with a paste of mineral oil and blue dye and heated using a power supply of 65 V. Still photographs were taken using a high-speed camera with a shutter speed of one-eighth of a second.

Results and Discussion

Lift and Drag Results

The NACA 0024 airfoil with a leading-edge rotating cylinder was tested at a chord Reynolds number of 6.5×10^4. The lift and pressure drag were calculated by the integration of the measured pressure distribution. The cylinder surface velocity ratio U_c/U is the parameter of prime importance in the present investigation. At large angles of attack, for example, $\alpha = 40$ deg, the wind-tunnel blockage due to the model is about 15% (Ref. 19). When the cylinder rotates, a new circulation, the Magnus effect, is induced around the airfoil, in addition to the circulation about the airfoil without the rotating cylinder. Therefore, the normal force acting perpendicular to the airfoil increases as the circulation induced by the rotating cylinder increases. The increase in the normal force results in an increase in the lift and would not affect the drag as long as the angle of attack is small. Experimental results showed that the effect of the leading-edge rotating cylinder becomes less at higher values of U_c/U.

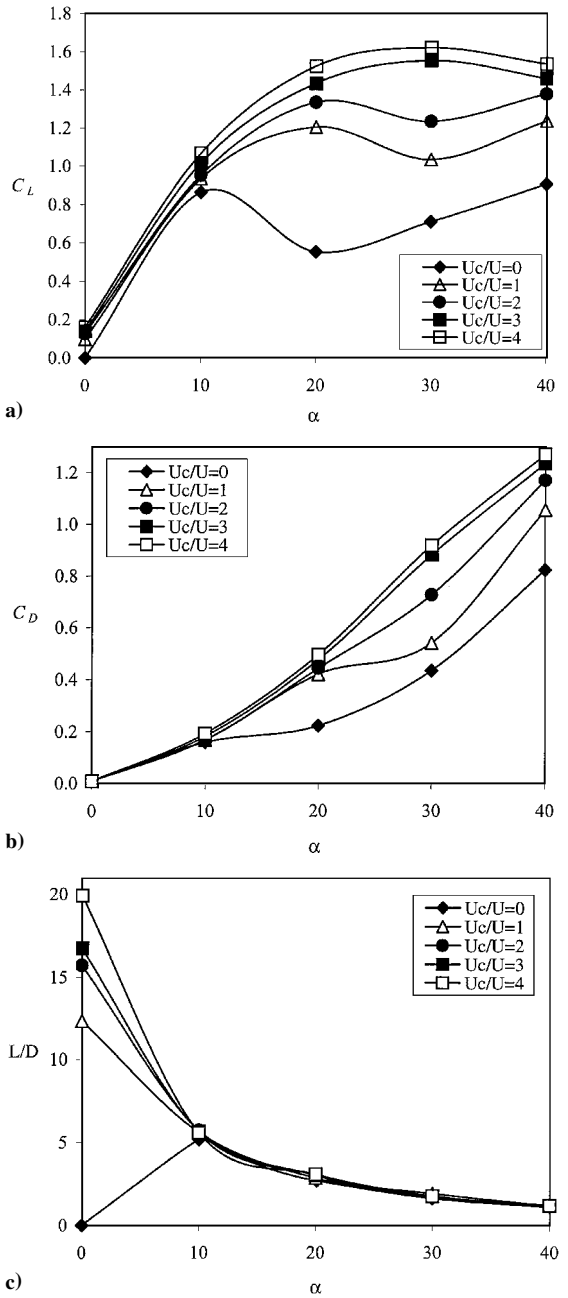

Fig. 2 Effect of leading-edge rotating cylinder at $\delta = 0$ on a) lift coefficient C_L, b) drag coefficient C_D, and c) lift-to-drag ratio L/D.

Figure 2a shows the lift coefficient plotted against angle of attack for different cylinder rotations. It is clear that the lift coefficient increases as the velocity ratio U_c/U increases. In the absence of rotation, the maximum lift coefficient is about 0.85. However, with the cylinder rotating at $U_c/U = 4$, the maximum lift coefficient is about 1.63. This shows an increase in the lift coefficient of about 92%. The slope of the lift coefficient curve remains unaffected. The rotating cylinder increases the stall angle of attack from around 10–15 deg at $U_c/U = 0$ to 30–35 deg at $U_c/U = 4$, which represents an increase of about 160%. Note that the curves for higher U_c/U reach a maximum, then they decrease gradually. At $\alpha = 40$ deg, the lift coefficient is about 1.46, which is quite remarkable. For a fixed-wing aircraft, this increase in lift coefficient and stall angle of attack would translate into improved maneuverability and performance of the airplane especially during STOL.

The variation of drag coefficient C_D with the angle of attack for different cylinder rotations is shown in Fig. 2b. The drag coefficient for the airfoil at $\alpha = 0$ deg for different U_c/U is insignificant. At $\alpha = 40$ deg, the maximum C_D varies from about 0.82 for $U_c/U = 0$ to about 1.24 for $U_c/U = 4$. The drag coefficient values are relatively high because the airfoil section is thick. Note that increasing the cylinder rotation directly increases the drag coefficient. This is because, when the cylinder rotates, the pressures on the upper surface of the airfoil decrease while the pressures on the lower surface increase. As a result, the normal force acting perpendicular to the airfoil increases and the drag will increase because the drag force is proportional to the sine component of the normal force, that is, $D \propto \sin\alpha$.

Because the lift-to-drag ratio is a measure of the aerodynamic efficiency of an airfoil, its variation is shown in Fig. 2c as a function of angle of attack for different U_c/U. Note that in the absence of any rotation, L/D is zero at $\alpha = 0$ deg due to the symmetry of airfoil. However, increasing the cylinder rotation to $U_c/U = 4$ results in an L/D value of around 20 for zero angle of attack. Note that the maximum L/D for the airfoil occurs at zero angle of attack. Therefore, the leading-edge rotating cylinder reduces the need for higher angles of attack.

The lifting characteristics of an airfoil equipped with a leading-edge rotating cylinder can be greatly enhanced by the use of high-lift devices such as a flap. Figure 3a summarizes the effects of a plain

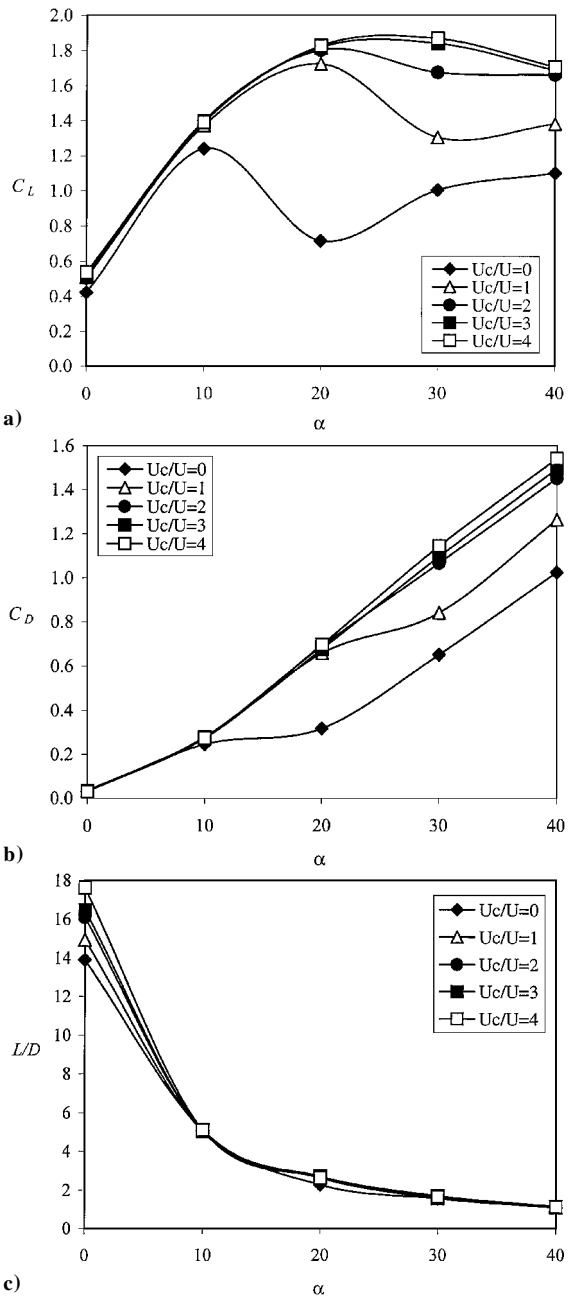

Fig. 3 Effect of plain flap at $\delta = 30$ deg on a) lift coefficient C_L, b) drag coefficient C_D, and c) lift-to-drag ratio L/D.

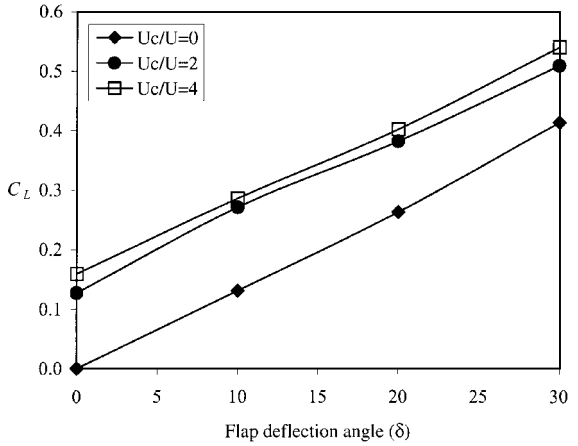

a) α = 0 deg

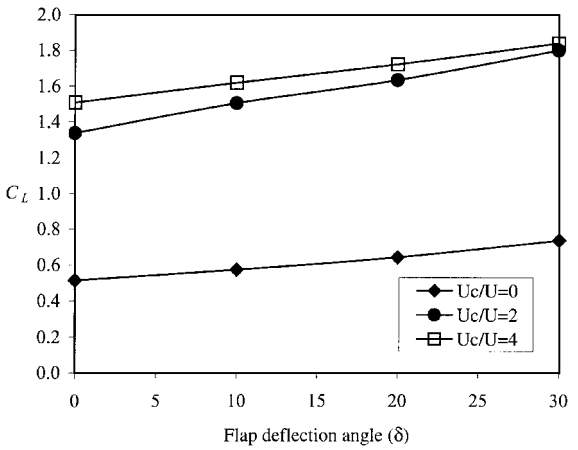

b) α = 20 deg

Fig. 4 Lift coefficient as a function of the flap deflection angle for different rotations.

flap deflected at $\delta = 30$ deg in the presence of cylinder rotation. In general, deflecting the flap is seen to shift the lift curve upward without affecting its slope. As seen in Fig. 3a, the highest section lift coefficient with the flap deflected and the cylinder stationary is 1.24. This value increases to 1.93 when the cylinder is rotated at $U_c/U = 4$. That is an increase in the maximum lift coefficient by about 56% (less than the 92% increase due to the cylinder rotation at $\delta = 0$). However, the total percentage increase in the maximum lift coefficient is about 130% due to the combined effects of $U_c/U = 4$ and $\delta = 30$ deg. Figure 3b shows the effect of the leading-edge rotating cylinder on the drag coefficient of the airfoil in the presence of the flap. As seen, the maximum drag coefficient is about 1.5 at $U_c/U = 4$ and $\alpha = 40$ deg. Also, Fig. 3b shows that C_D increases as U_c/U increases, which can be considered as a penalty representing the power required to drive the cylinder. Moreover, the deflection of the flap resulted in the reduction of the L/D ratio of the airfoil by about 10%, as shown in Fig. 3c.

Figures 4a and 4b present the lift coefficient as a function of the flap deflection angle for different rotation speeds at $\alpha = 0$ and 20 deg, respectively. Note that the lift coefficient varies almost linearly with the flap deflection angle for a specific rotation. Also, the cylinder rotation has a small effect on the slope of the lift curve with respect to the flap angle C_{L_δ}.

Boundary-Layer Results

Miniature single hot-wire probes were used to survey the velocity fluctuations at different positions. Figure 5 shows the effect of the cylinder rotation on the velocity profiles, u/U, for $\alpha = 0$ deg at five streamwise stations, $x/c = 0.2$, 0.4, 0.6, 0.8, and 1.0. For comparison, the velocity profiles for two cases, $U_c/U = 0$ and 4, are shown together in Fig. 5 to illustrate the effects of the moving surface on the development of the boundary-layer flow. Near

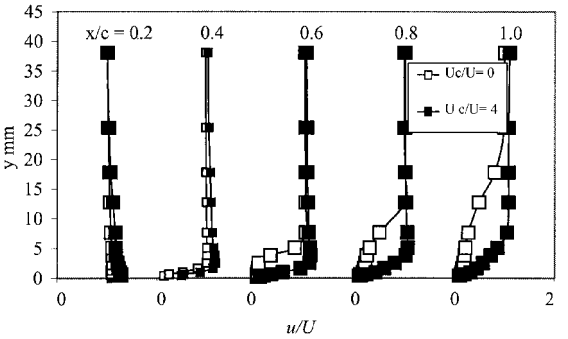

Fig. 5 Effect of leading-edge rotating cylinder on velocity profiles on the upper surface of the airfoil.

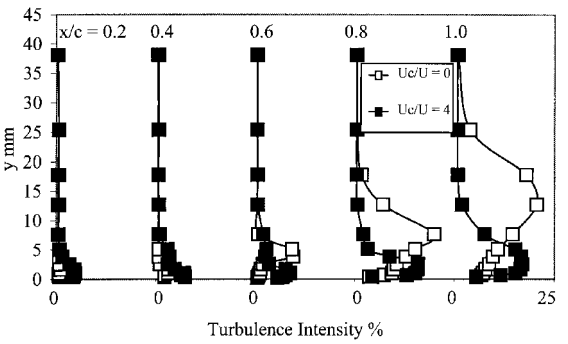

Fig. 6 Effect of the leading-edge rotating cylinder on turbulence intensity on the upper surface of the airfoil.

the leading edge of the airfoil, $x/c = 0.2$, the velocity distribution is almost uniform. Noted that the presence of cylinder rotation reduces the boundary-layer thickness and causes the boundary layer to adhere to the surface of the airfoil. The effect of the cylinder rotation is felt farther at the trailing edge of the airfoil. In the absence of any rotation, the boundary layer has a thickness of 3 mm at $x/c = 0.4$ and grows to about 25 mm at $x/c = 1.0$. However, at $U_c/U = 4$, the boundary-layer thickness grows from 1.5 mm at $x/c = 0.4$ to 7.0 mm at $x/c = 1.0$.

The turbulence intensity u'/U, for $U_c/U = 0$ and 4, are shown in Fig. 6. In the absence of cylinder rotation, the turbulence intensity has a maximum value of 20% at $x/c = 1.0$ and a value of 15% for $U_c/U = 4$ at the same streamwise location. Note that, at $x/c \geq 0.6$, the turbulence intensity is higher for the $U_c/U = 0$ case than for the case of $U_c/U = 4$. This increase is likely to be due to the adverse pressure gradient to which the boundary layer is subjected[20] for the case of $U_c/U = 0$.

Flow Visualization Results

The smoke-wire technique was used to visualize the flow around the model. The flow visualization photographs shown in Figs. 7 and 8 give an image of the flow conditions that exist on the upper surface of the airfoil at various angles of attack for different cylinder rotations. Figures 7a and 7b show the streamlines for the airfoil at $\alpha = 10$ deg for $U_c/U = 0$ and 1, respectively. For $U_c/U = 0$, one can see that the airfoil is under trailing-edge separation (Fig. 7a). However, with the cylinder rotating at $U_c/U = 1$, the flow becomes attached.

Figures 8 show the flow pattern over the airfoil at $\alpha = 20$ deg. At $U_c/U = 0$, the flow over the upper surface of the airfoil is completely separated. Increasing the cylinder rotation to $U_c/U = 1$ delays the separation but does not cause complete reattachment. As the cylinder rotates at higher U_c/U, the size of the wake behind the airfoil diminishes until the flow becomes completely attached to the upper surface of the airfoil at $U_c/U = 3$–4 (see Figs. 8d and 8e). Similar trends persist at $\alpha = 30$ and 40 deg. Note that complete reattachment of the boundary layer was not achieved for $\alpha = 40$ deg. By the consideration of the changes in the flow patterns shown in Figs. 7 and 8, the required rotation of the cylinder $(U_c/U)_R$ to reattach the flow is shown in Table 1.

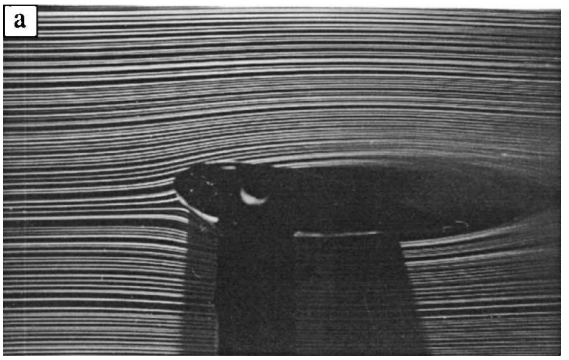

$U_c/U = 0$

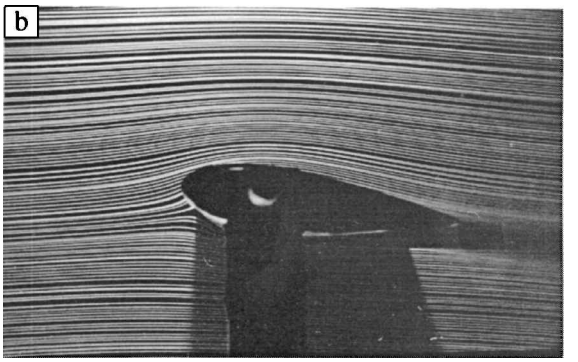

$U_c/U = 1$

Fig. 7 Flow visualization photographs, $\alpha = 10$ deg.

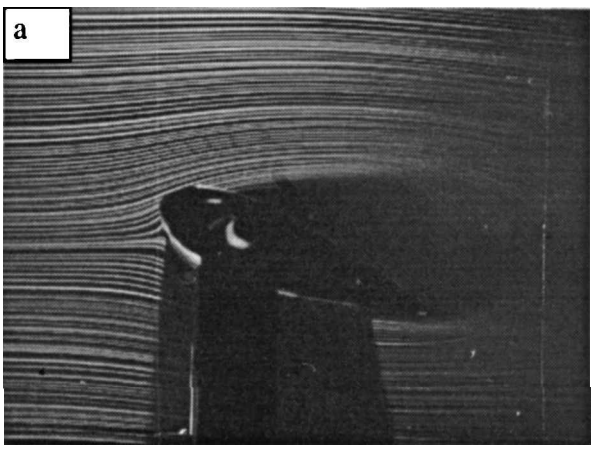

$U_c/U = 0$

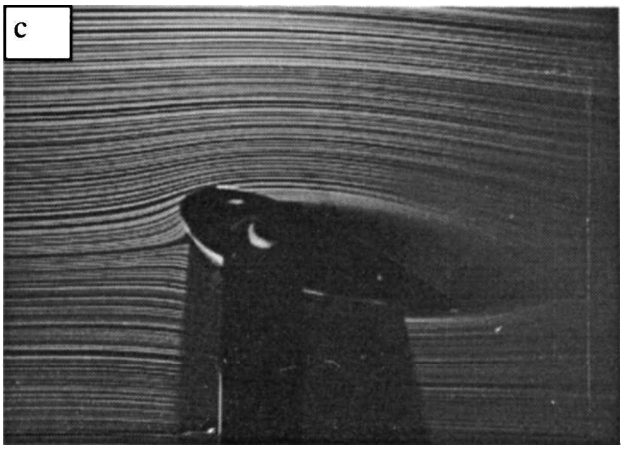

$U_c/U = 2$

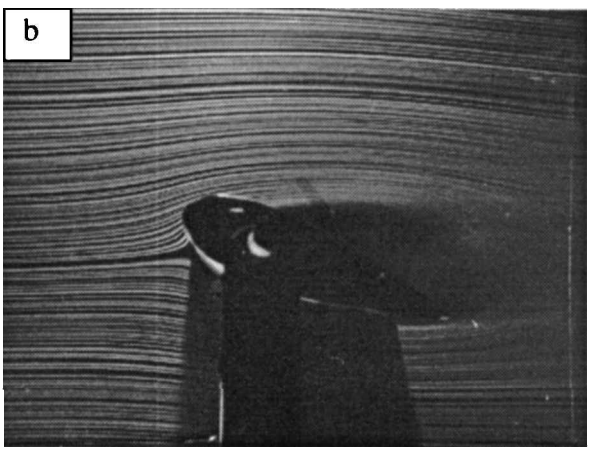

$U_c/U = 1$

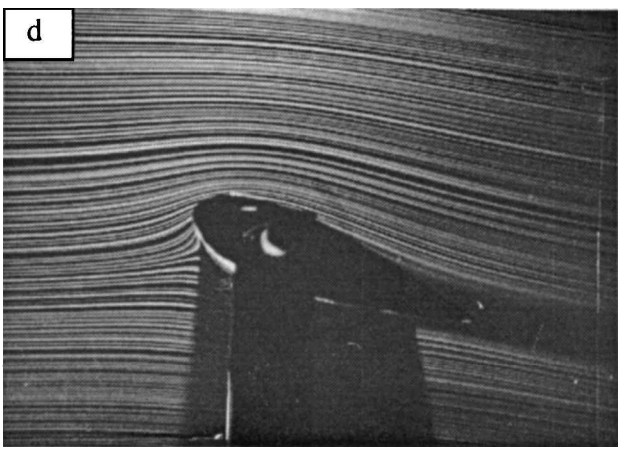

$U_c/U = 3$

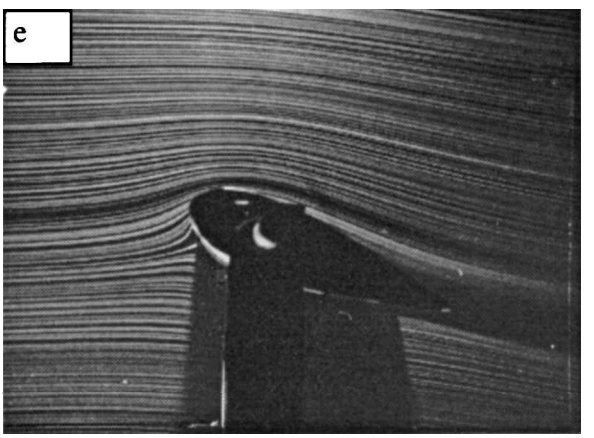

$U_c/U = 4$

Fig. 8 Flow visualization photographs at $\alpha = 20$ deg.

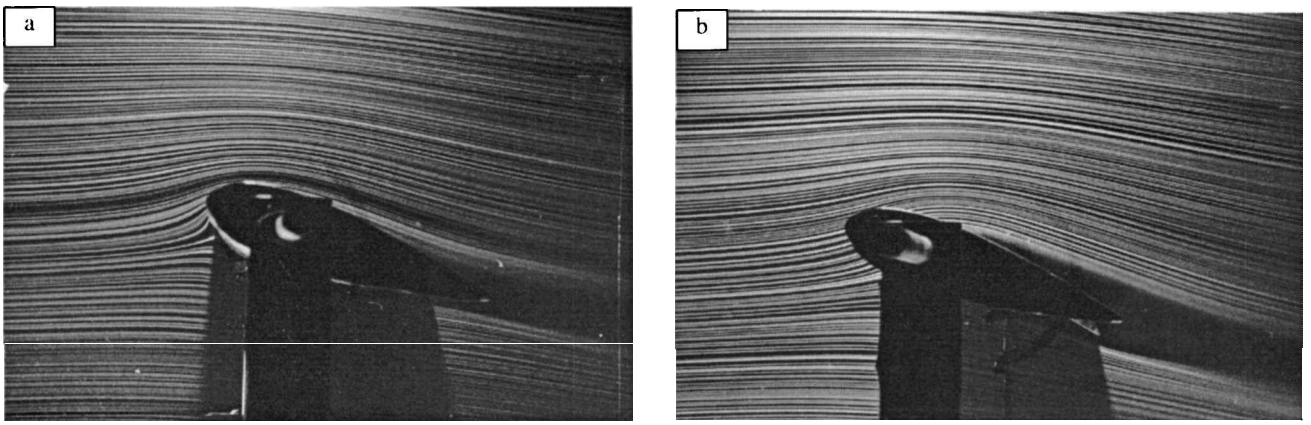

δ = 0 deg δ = 30 deg

Fig. 9 Flow visualization photographs for the case of U_c/U = 4 and α = 20 deg.

Table 1 Flow reattachment at different angles of attack as a function of U_c/U

Angle of attack	$(U_c/U)_R$
10	1
20	3
30	≥ 4
40	>4

The effect of the flap on the flow pattern over the upper surface of the airfoil is shown in Fig. 9. Note that the deflection of the flap moves the separation point upstream toward the leading edge of the airfoil.

Conclusions

The wind-tunnel test program shows that the leading-edge rotating cylinder is a successful device in increasing the sectional lift coefficient and lift-to-drag ratio at low angles of attack, hence reducing the need for higher angles of attack. Also, with high-speed rotation of the cylinder, the stall has been delayed. The increase in the lift coefficient and the delay in the stall angle of attack were about 92 and 160%, respectively. In addition, the lift-to-drag ratio increased from 0 to a value of around 20 at zero angle of attack, hence reducing the need for higher angles of attack for STOL. This increase in the lift coefficient, lift-to-drag ratio, and stall angle of attack would make an airplane fitted with such an airfoil more maneuverable and improve its performance in terms of STOL. Note that increasing the cylinder rotation would increase the drag coefficient. It also has a small effect on the slope of the lift curve with respect to the flap deflection angle.

Although the flap was successful in increasing the lift coefficient, it reduced the lift-to-drag ratio of the leading-edge rotating cylinder airfoil. Results of the boundary-layer measurements showed that the leading-edge rotating cylinder reduced the boundary-layer thickness and the turbulence intensity in the vicinity of the airfoil surface. The flow visualization studies showed that an increase in the speed of the leading-edge rotating cylinder would delay the separation on the upper surface of the airfoil or perhaps forces the flow to reattach. Considering the changes in the lift coefficient vs U_c/U, along with flow visualization results, suggests that the effect of the leading-edge rotating cylinder becomes less at higher U_c/U.

Acknowledgment

The authors would like to acknowledge the support of King Fahd University of Petroleum and Minerals, Dhahran, Saudi Arabia.

References

[1]Schlichting, H., *Boundary Layer Theory*, McGraw–Hill, New York, 1968.

[2]Chang, P. K., *Separation of Flow*, Pergamon, Oxford, England, U.K., 1970.

[3]Prandtl, L., and Tietjens, O. G., *Applied Hydro- and Aero-Mechanics*, McGraw–Hill, New York, 1934.

[4]Alvarez-Calderon, A., and Arnold, F. R., "A Study of the Aerodynamic Characteristics of a High Lift Device Based on Rotating Cylinder Flap," TR RCF-1, Stanford Univ., Stanford, CA, 1961.

[5]Cook, W. L., Hickey, D. H., and Quigley, H. C., "Aerodynamics of Jet Flap and Rotating Cylinder Flap STOL Concepts," Paper 10, AGARD Fluid Dynamics Panel on V/STOL Aerodynamics, Delft, The Netherlands, April 1974.

[6]Cichy, D. R., Harris, J. W., and MacKay, J. K., "Flight Tests of a Rotating Cylinder Flap on a North American Rockwell YOV-10 Aircraft," NASA CR-2135, Nov. 1972.

[7]Tennant, J. S., "The Theory of Moving Wall Boundary Layer Control and its Experimental Application to Subsonic Diffusers," Ph.D. Dissertation, Clemson Univ., Clemson, SC, May 1971.

[8]Jonhson, W. S., Tennant, J. S., and Stamps, R. E., "Leading-Edge Rotating Cylinder for Boundary-Layer Control on Lifting Surfaces," *Journal of Hydronautics*, Vol. 9, No. 2, 1975, pp. 76–78.

[9]Tennant, J. S., Jonhson, W. S., and Krothapalli, A., "Rotating Cylinder for Circulation Control on an Airfoil," *Journal of Hydronautics*, Vol. 10, No. 3, 1976, pp. 102–105.

[10]Tennant, J. S., and Yang, T., "Turbulent Boundary-Layer Flow from Stationary to Moving Surfaces," *AIAA Journal*, Vol. 11, No. 8, 1973, pp. 1156–1160.

[11]Tennant, J. S., Jonhson, W. S., and Keaton, D. D., "Boundary-Layer Flows from Fixed to Moving Surfaces Including Gap Effects," *Journal of Hydronautics*, Vol. 12, No. 2, 1978, pp. 81–84.

[12]Sayers, A. T., "Lift Coefficient and Flow Visualization on Leading Edge Rotating Cylinder Rudder," *International Journal of Mechanical Engineering Education*, Vol. 7, No. 2, 1979, pp. 75–79.

[13]Hassan, A. A., and Sankar, L. N., "Separation Control Using Moving Surface Effects: Numerical Simulation," *Journal of Aircraft*, Vol. 29, No. 1, 1992, pp. 131–139.

[14]Brooks, J. D., "The Effect of a Rotating Cylinder at the Leading and Trailing Edges of a Hydrofoil," U.S. Naval Ordnance Test Station, NAVWEPS Rept. 8042, April 1963.

[15]Modi, V. J., Sun, J. L. C., Akutsu, T., Lake, P., McMillan, K., Swinton, P. G., and Mullins, D., "Moving-Surface Boundary-Layer Control for Aircraft Operation at High Incidence," *Journal of Aircraft*, Vol. 18, No. 11, 1981, pp. 963–968.

[16]Modi, V. J., Mokhtarian, F., Fernando, M. S. U. K., and Yokomizo, T., "Moving Surface Boundary-Layer Control as Applied to Two-Dimensional Airfoils," *Journal of Aircraft*, Vol. 28, No. 2, 1991, pp. 104–112.

[17]Modi, V. J., Munshi, S. R., Bandyopadhyay, G., and Yokomizo, T., "High-Performance Airfoil with Moving Surface Boundary-Layer Control," *Journal of Aircraft*, Vol. 35, No. 4, 1998, pp. 544–553.

[18]Batill, S. M., and Mueller, T. J., "Visualization of Transition in the Flow over an Airfoil Using the Smoke-Wire Technique," *AIAA Journal*, Vol. 19, No. 3, 1981, pp. 340–345.

[19]Rae, W. H., and Pope, A., *Low-Speed Wind Tunnel Testing*, Wiley, New York, 1984.

[20]Fernholz, H. H., "External Flows," *Turbulence*, edited by P. Bradshaw, Springer–Verlag, Berlin, 1978.